Energy Conversion and Management: X 23 (2024) 100634

Contents lists available at ScienceDirect

Energy Conversion and Management: X

journal homepage: www.sciencedirect.com/journal/energy-conversion-and-management-x

Transient analysis of an efficient solar assisted air-conditioning system for subtropical climate with various solar thermal collectors

Ghulam Qadar Chaudhary [a], Muhammad Waheed Azam [b,*], Fabio Bozzoli [b], Uzair Sajjad [c], Pamela Vocale [b], Luca Cattani [b], Rasoul Fallahzadeh [b]

[a] Mechanical Engineering Department, MUST, Mirpur 10250 AJK, Pakistan
[b] Department of Architecture and Engineering, University of Parma, Parco Area delle Scienze 181/A, 43124 Parma, Italy
[c] Interdisciplinary Research Center for Sustainable Energy Systems (IRC-SES), King Fahd University of Petroleum and Minerals, Dhahran, Saudi Arabia

ARTICLE INFO

Keywords:
Solar air-conditioning
Desiccant cooling
Regenerative evaporative cooling
Maisotsenko cycle cooler
Solar thermal collectors
Transient analysis
TRNSYS

ABSTRACT

The air conditioning demand of the world is largely fulfilled by vapor compression systems; however, these systems are also responsible for depleting ozone layer due to the nature of refrigerants. Desiccant cooling systems integrated with solar thermal energy technologies could be an attractive alternative with some performance enhancement techniques. In this study, transient seasonal performance investigation is performed for an innovative solar integrated desiccant cooling system that uses regenerative evaporative cooler known as solar assisted desiccant integrated Maisotsenko cycle cooler for better cooling performance. Furthermore, transient annual performance analysis of solar system for meeting thermal energy requirement for regenerating the desiccant wheel in summer season and handling heating load of the building in winter season is also carried out with three different solar thermal collector technologies for finding out more efficient technology. The key performance indicators in this study are useful energy gain, solar source efficiency, auxiliary energy sharing, coefficient of performance, and solar fraction. The results of the key performance parameters are reported as monthly average values. The proposed integrated system resulted to be very efficient with a maximum COP value of 1.13 in April when latent cooling loads are low and 0.78 in August when latent cooling loads are higher. The system's maximum cooling capacity is 24 kW in April corresponding to a sensible heat factor of 0.720. Furthermore, the regeneration temperature requirements ranged from 50 °C to 78 °C, respectively that makes it favorable to use low grade thermal energy through non concentrating solar thermal collectors. The regeneration thermal energy requirement for desiccant wheel fluctuates throughout the year, maximizing in August due to higher dehumidification requirements. The study also revealed that the evacuated tube collector technology is most suitable with average annual efficiency of around 36 %.

1. Introduction

Air conditioning utilizes a substantial amount of electricity in many residential and commercial buildings [1]. Due to global warming impact, there is a steadily growing demand of energy for air conditioning applications. Air conditioning requirements are typically met by conventional vapor compression refrigeration systems. In vapor compression refrigeration systems, CFCs and HFCs refrigerants are mostly used which pollute the environment and cause ozone layer depletion [2]. Moreover, as most of the electricity generation relies on fossil fuels vapor compression systems are also indirectly contributing in carbon emissions.

Direct Evaporative cooling is an environmentally friendly and energy-saving air conditioning method; however, its performance is strongly decreased when utilized in hot and humid climates [3,4]. There are two main types of evaporative cooling techniques that are used in desiccant cooling systems: indirect evaporative cooling and direct evaporative cooling [5]. In direct evaporative cooling, there is direct contact between air and water as a result the temperature of the air is reduced, but the humidity level increases up to 90 % [6]. In an indirect evaporative cooler, there is no direct contact between the primary (product) air and the secondary air. Due to water evaporation on the wet side, heat passes from the product air to the working air. As a result, the IEC heat exchanger can cool the product air without introducing moisture, however, COP of such systems is lower as compared to direct

* Corresponding author.
E-mail address: muhammadwaheed.azam@unipr.it (M. Waheed Azam).

https://doi.org/10.1016/j.ecmx.2024.100634
Received 10 January 2024; Received in revised form 29 April 2024; Accepted 20 May 2024
Available online 24 May 2024

Nomenclature

A	Area, m^2
AES	Auxiliary energy share, *kWh*
CFCs	Chloro-fluoro-carbons
COP	Coefficient of Performance
C_{pw}	Heat Capacity, kJ/(kg. K
c_p	Specific heat of fluid, kJ/(kg. K
DEC	Direct evaporative cooler
G	Global radiation, W/m^2
GSHF	Grand sensible heat factor
HFCs	Hydro fluorocarbons
HVAC	Heating ventilation and air conditioning
IEC	In-direct evaporative cooler
MC	Maisotsenko cycle
Q	Thermal Energy, kW
Q_{sol}	Solar energy, W/m^2
Q_t	Total energy kW
q	Air volume flow, m^3
RMSE	Root means square error
SDI-MC	Solar desiccant integrated Maisotsenko Cycle
SHF	Sensible heat factor, *%*
SF	Solar fraction, *%*
SWHS	Solar water heating System
T	Temperature, °C
T_{amb}	Ambient temperature, °C
T_{reg}	Regeneration temperature, °C
T_{sin}	Process inlet temperature, °C
T_{sout}	Process outlet temperature, °C
T_{zone}	Zone temperature, °C
ω_{reg}	Humidity ratio of regeneration air at inlet, g/kg
ω_{sin}	Humidity ratio of process air at inlet, g/kg
ω_{sout}	Humidity ratio of process air at outlet, g/kg
ω_{zone}	Humidity ratio of zone, g/kg

Greek Letter

η	Efficiency
ρ	Density

Subscripts

aux	Auxiliary
c	Collector
d	Demand
in	Inlet
lat	Latent
out	Outlet
reg	Regeneration
sen	Sensible
t	Total
w	Water
wds	Water in desiccant system

evaporative coolers and both type of coolers can only cool the incoming stream of the air up to its wet bulb temperature [7].

The regenerative evaporative cooler like Maisotsenko cycle cooler is an improved design of in-direct evaporative cooling that can lower the temperature of incoming stream of air up to its dew point [8]. However, all types of evaporative coolers suffer serious performance limitations especially when used in hot and humid climate conditions therefore, integrated with desiccant dehumidifier to remove the moisture content of the air.

The solar desiccant integrated cooling system is an attractive alternative to meet the air conditioning demand for human comfort. This system has great potential to save primary energy consumption as compared to vapor compression refrigeration system [9]. With the ability to lower carbon emissions and improve sustainability, solar energy is an attractive choice and alternative when it comes to supplying energy needs in an eco-friendly way. There are various studies that involve the efficiency enhancement of the sustainable cooling systems by using various techniques [10–12].

Many researchers and scientists have investigated the desiccant cooling systems like experimental performance evaluation of desiccant coated heat exchangers from a combined first and second law of thermodynamics perspective and revealed that the requirement for regeneration temperature rises, the system's COP decreases. It was reported that the system's COP at 70 °C regeneration temperature was 2 [13]. Similarly, another simulation-based transient analysis of solar desiccant cooling system was carried out for hot, humid, and semi-humid conditions. In hot and humid conditions, the system achieved the highest COP of 0.728 [14]. A simulation study on desiccant cooling system with different configurations in the TRNSYS platform in the climate conditions of Pakistan. An auxiliary heater was installed in the cooling loop to heat the return air to the required temperature to achieve the optimum regeneration temperature. Results indicated that the best-performing systems required a bigger collector area to enhance the regeneration temperature of the desiccant wheel [15].

Furthermore, the simulation-based study by using TRNSYS software for a thermal hybrid photovoltaic panel's solar cooling system revealed that the hybrid photovoltaic system annual efficiency was 31.7 % and the system payback period was 4.6 years [16]. A similar study on transient analysis where simulation model of the building was developed using Energy Plus software in the climate condition of different cities in Australia, implementing a desiccant cooling system, 121 tons less CO_2 were released into the atmosphere. The coefficient of performance (COP) of the desiccant evaporation cooling system was 7 with the highest and lowest yearly building load of 300 MW and 180 MW, respectively [17].

Another simulation and experimental study of the solar hybrid desiccant cooling system in the climate conditions of four different cities in Pakistan. A model for a pre-cooled solar hybrid desiccant cooling system was developed using TRNSYS software, and it was subsequently verified through experimental data. The pay-back period of solar collectors for environmental and energy systems was 1.50 and 1 year. It was reported that Lahore city achieved human comfort conditions during the cooling season without auxiliary energy for about three months [18].

The solar desiccant cooling system was designed and analyzed during the summer season. It was reported that the system's COP ranges from 0.65 to 1.17, with a collector efficiency of 45 % [19]. The performance of the desiccant wheel depends on regeneration temperature and outside conditions. The COP of the system varies from 0.38 to 0.40 in moderate humid climate conditions. The desiccant cooling system utilized vacuum tube collectors as its solar thermal sources, with the vacuum tube collector achieving an efficiency of 0.60 [20]. An experimental-based study for the solar desiccant cooling system in the hot climate of Europe revealed the coefficient of performance of the solar desiccant cooling system was 2 [21]. Similarly, performance analysis of the desiccant cooling system by developing an artificial neural network model under a wide range of inlet conditions. The performance of the artificial neural model was compared with the output of the system. The results revealed that when the moisture removal capability is negatively affected by increasing the ambient temperature [22]. In another study focused on performance evaluation of solar water heating system using a parabolic trough comprising of aluminum-coated channel tubes with a copper-dimpled tube. The results showed that a mass flow rate of 2.5 kg/min gives the best results, with a total thermal efficiency of 31.85 % with 11 % enhancement in efficiency as compared to plain tube geometry [23].

A significant research gap is the absence of transient analysis of solar integrated desiccant cooling systems using regenerative evaporative cooler i.e. Maisotsenko cooler in the current literature. Furthermore, this study also helps to select the most suitable solar thermal system for its application with solar assisted air-conditioning application. Moreover, the developed simulation model acts as a tool to investigate the performance of the said system in any climate of the World and any modified system or control strategy to evaluate the performance of the sustainable desiccant cooling systems. Addressing these gaps will advance the field of sustainable energy solutions by improving our understanding of system dynamics and making it easier to use solar energy more effectively for cooling applications. The objective of this research is to investigate several critical aspects of the SDI-MC system, including its solar fraction, useful energy gain, auxiliary energy sharing, and coefficient of performance. The research also highlights the most efficient solar thermal collectors among evacuated tubes, parabolic troughs, and flat plate collectors. In conclusion, this study enhances ongoing research to enhance sustainable energy use and minimize our reliance on nonrenewable sources of energy.

2. Method and materials

The simulation based transient seasonal performance analysis of an innovative solar desiccant integrated air-conditioning system is carried out through TRNSYS software for hot and humid climate conditions of Pakistan. Initially, an office building model is developed keeping in view the average size of an office space using TRNBUILD and google SketchUp software with proper assumptions and commonly used building materials. Afterwards, the parameters are assigned along with occupancy lighting schedule, infiltration rates, thermal energy gain through glazing etc. Afterwards, the simulation model of an innovative solar integrated desiccant cooling system was also developed in TRNSYS studio and hourly dynamic buildings loads are applied on the system. The complete simulation model was simulated for climate conditions of Taxila Pakistan characterized as hot and humid climate. The results of the simulation model are validated with the authors indigenously developed experimental test rig for wide range of operating conditions. simulations are repeated three times by incorporating first section is a detailed introduction to TRANSYS software and its components which are used in the designing of the SDI-MC system, while in the second section, the procedure and method of modelling are explained.

2.1. Introduction of TRNSYS software

TRNSYS is based on a modular approach to investigate the transient performance of different renewable energy systems and developed by Solar Energy Laboratory at the University of Wisconsin in 1977 [24]. The TRNSYS software is programmed in Fortran and is known as the TRN.exe extension. The project is developed in TRNSYS with the help of modules and components found in its built-in library. However, it has capability to simulate various other customized mathematical models of components in Engineering Equation Solver, and MATLAB [25].

TRNBuild is used to create input detail for multi-zone buildings and permits to enter all the building structure data as well as simulate the thermal performance of the building (e.g., Windows optical properties, cooling, and heating seasons). TRNSYS software has a special extension TRNEdit that can primarily be used to generate TRNSYS input files. Moreover, TRNSYS software consists of various programs such as TRANSED which is an application of TRNEdit [26].

2.2. Development of building model

An office building model is developed in the Google SketchUp software. It is a 3D modelling program that is used for drawing applications [27]. This model consists of three offices, reception area, working area, kitchen, and baths as shown in Fig. 1.

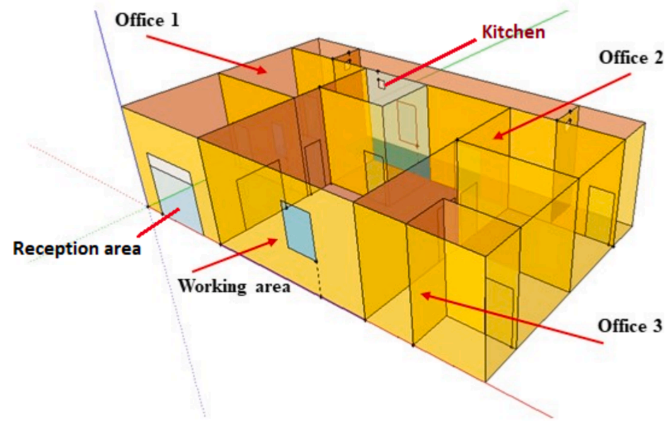

Fig. 1. Office building model in google SketchUp.

Table 1
Characteristics of building zone.

Sr. #	Zone	Area (m^2)	Volume (m^3)
1	Office 1	15.5	55
2	Office 2	16	58
3	Office 3	13	47.5
4	Co-Working space	44	160
5	Kitchen	7	33

Table 2
Model assumptions and material properties.

Roof	Geometry	Plain horizontal
	Value of U	2.46 W/m^2k
External Wall	Geometry	Plain Vertical
	Value of U	0.727 W/m^2k
Doors	Value of U	1.4 W/m^2k
	Thickness	0.01 m
Windows	Glazing ratio of façade	5 %
	U-value	2.8 W/m^2 K
	Shadowing devices	N. A
	Frame area	13 %
Room	Habitable surface	80 %
	Internal gains	23 kWh /m^3 k
	heating coefficient	0.95
	Thermal capacity of air	0.34 W/m^3K
	Inner temperature	19 °C
	Ventilation	0.5 h^{-1}

The building zone specification is shown in Table 1.

Office 1 is partitioned to accommodate a receptionist. Building envelop properties of each zone were defined in TRNBuild program. All surfaces (walls, floor, roof, doors, windows etc.) were defined in layers according to local construction practice. Table 4.2 describes the construction of walls used in the building envelope. The building design parameters have thoroughly considered the Building Energy Codes of Pakistan All building zones including windows, walls, doors, floors, and roofs are clearly defined with the following particulars as mentioned in Table 2.

Table 3
Characteristics of building windows and doors.

Sr. #	Zone	Area (m^2)	U value (W/m^2K)
1	Window (Kitchen)	0.76	2.89
2	Window (working area)	1.86	2.89
3	Door (Main entrance)	3.90	4.20

Commonly available double glass windows such as ASH140 DBLE – MOD have been used having 3.2 mm thick glass with aluminum frames. Similarly, a single glass 10 mm thick door is used for each zone entrance. The internal glass doors are glazed for privacy and it is assumed that their role of light transmittance from one zone to other is negligible, however external main door is unglazed. The specifications of windows and external door are described in Table 3.

2.3. Thermal load analysis for building load

The inputs in TRNBuild program can be defined as constant values, schedules or set as inputs. The inputs are then defined in the TRNSYS studio. Occupancy, lighting, heating cooling and infiltration are defined in TRNBuild program as shown in Fig. 2.

The occupancy and lighting schedule of living zones is defined as schedule filtration and heating/cooling set points are considered as inputs from studio. The occupancy of the building is assumed to be fixed with 17 people. The lighting schedule is active from 9:00 AM to 5:00 PM comprising of 350 W thermal load.

2.4. Building occupancy and air-conditioning set points

The occupancy schedule of all zones was different and defined separately in TRNBuild program. Fig. 3 shows the occupancy schedule of all living zones. Offices share the same schedule. Whereas the reception area is assumed to have three people during office time.

Heating/cooling set points were defined in the studio by using seasonal, daily controls. When heating or cooling was required during office times (9–5 pm) as shown in Fig. 4 in the zones the temperature was set to 25 °C otherwise 0 °C.

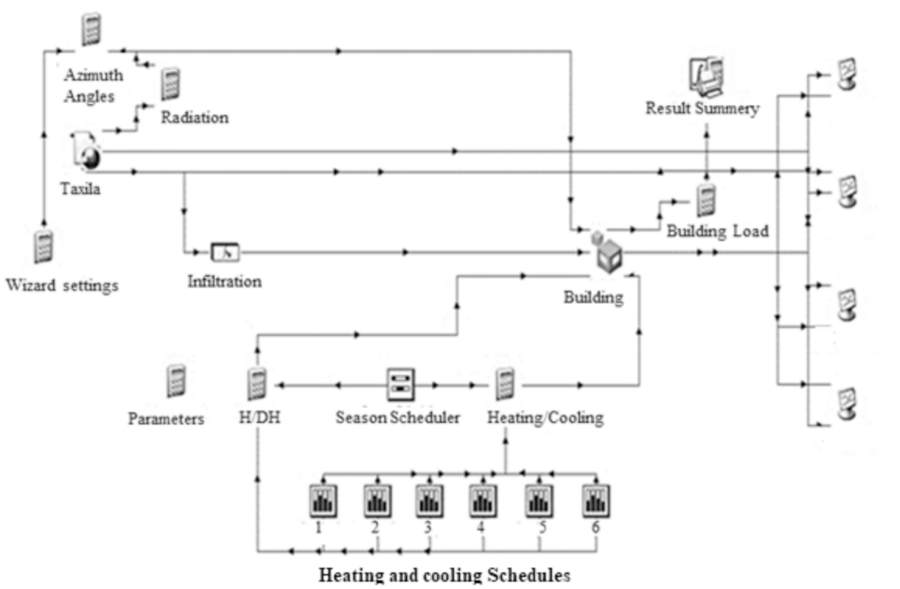

Fig. 2. TRNSYS model for simulating the building hourly dynamic loads.

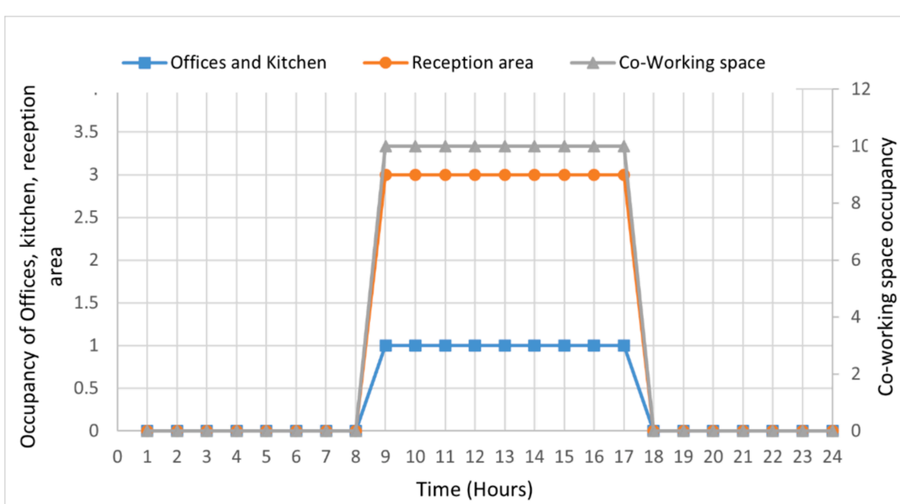

Fig. 3. Occupancy schedule of office building.

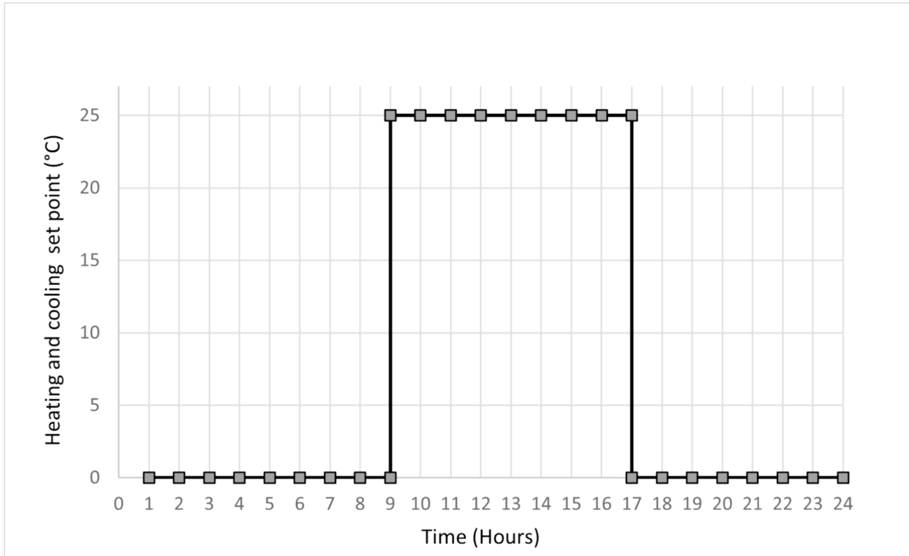

Fig. 4. Heating and cooling set point.

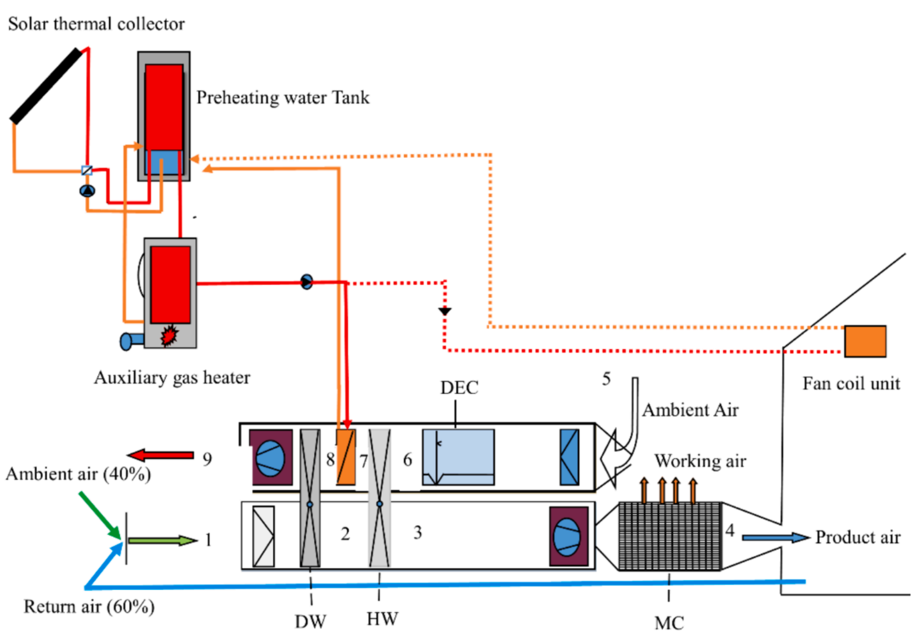

Fig. 5. Schematic representation of SDI-MC system.

2.5. Overview of the solar-assisted desiccant integrated Maisotsenko cooler

This system can be classified into two sub-systems such as solar water heating system and desiccant integrated Maisotsenko cycle cooling system. The schematic representation of both systems is shown in Fig. 5.

2.5.1. Solar water heating system

A solar water heating system (SWHS) is used to produce hot water that is passed through water to air heat exchanger to produce hot air to regenerate desiccant wheel. In this research, three different types of solar collectors were analyzed to find the most efficient and suitable technology for solar assisted air-conditioning. The SWHS consists of a hot water storage tank, solar thermal collectors, a conventional water heater with auxiliary heater, and different types of sensors i.e. (temperature, humidity, and pressure). In the absence of solar energy, the regeneration temperature for the desiccant wheel is maintained by an auxiliary storage tank. Storage tanks are also used for water storage and circulation of water. When the temperature is increased above 60 °C the water is supplied from the storage tank to the conventional water heater. The storage tank is a backup source to full fill the temperature requirements.

2.5.2. Desiccant system integrated with Maisotsenko cycle cooler in recirculation mode

The Desiccant integrated Maisotsenko cooling system in recirculation mode is shown in Fig. 5. The desiccant cooling system consists of two chambers i.e., the process side, and the regeneration side. The desiccant wheel is an important component in the desiccant cooling system that efficiently controls the process of air humidity. Moreover, the shape of the desiccant wheel is like a honeycomb and this structure is mostly preferred as it offers less air pressure drop during operation. On

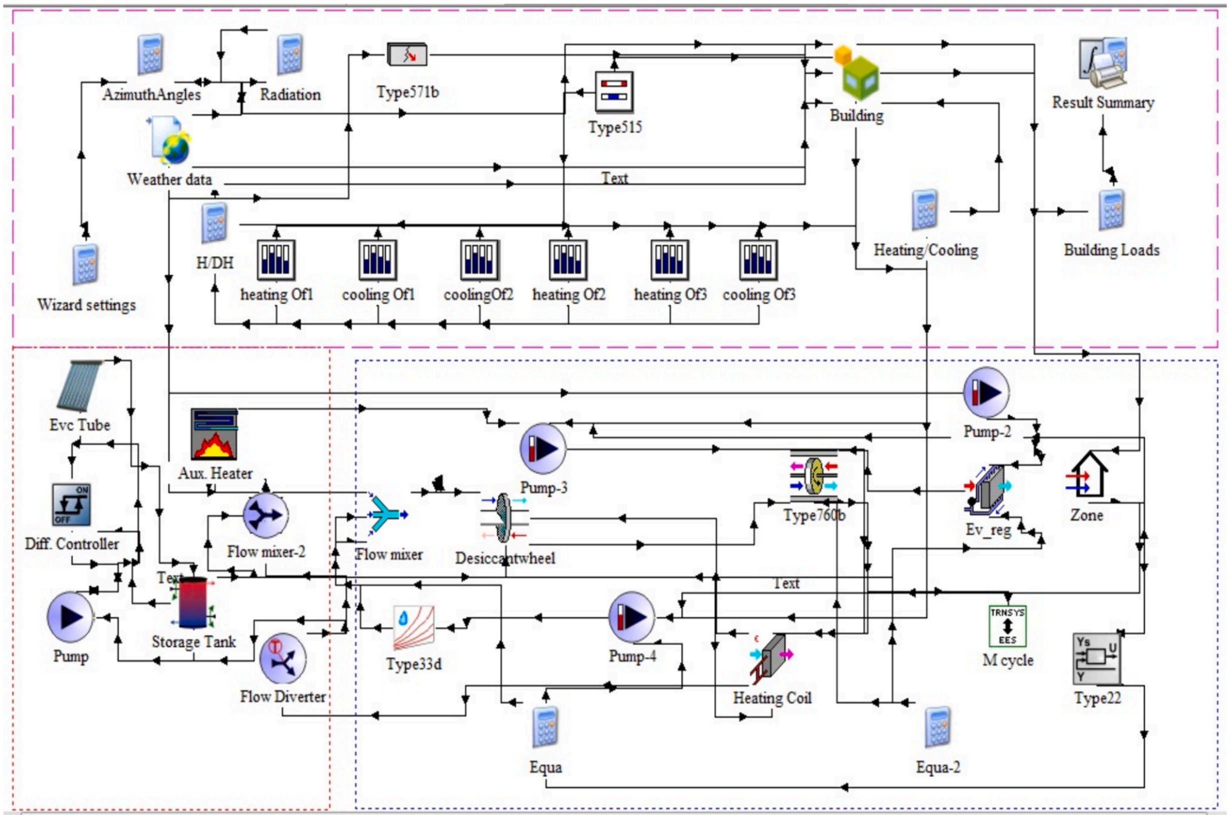

Fig. 6. Simulation studio interface for building integrated sdi-mc model.

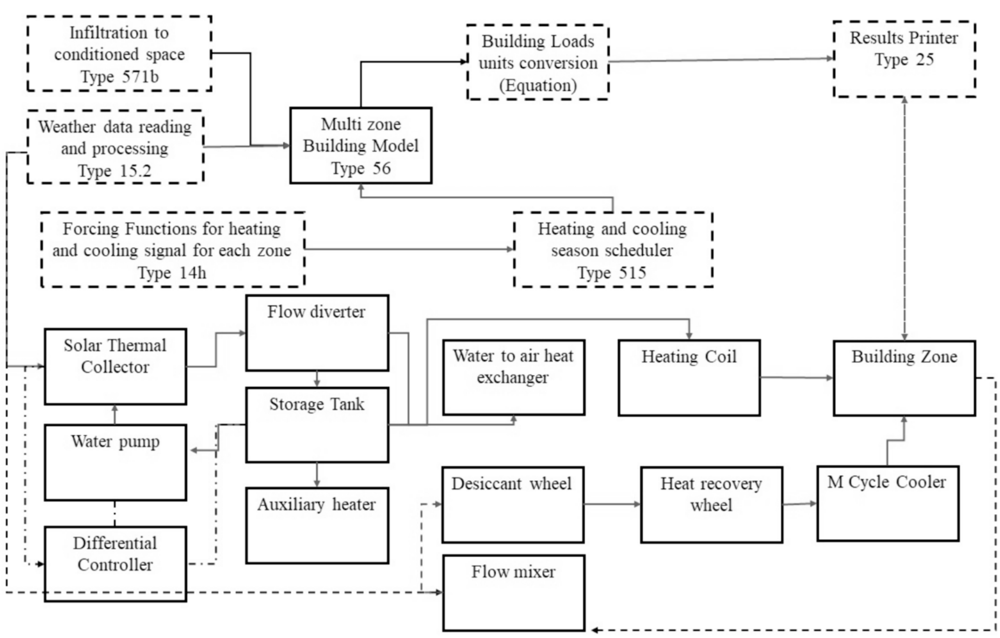

Fig. 7. Information flow diagram of TRNSYS Model.

the process side, the air (60 % return air from conditioned space and 40 % ambient air) is passed through desiccant wheel for moisture absorption. The rotation of the desiccant is at a very low speed. The desiccant wheel absorbed the moisture content from the air due to the partial pressure difference between the desiccant material and the moisture content present in the process air.

Afterward, the air passes through the heat recovery wheel from the 2–3 stage resulting in the supply air stream being pre-cooled. During this process, the temperature of the air decreases. In the next stage 3–4, air is introduced into Maisotsenko cycle cooling system for sensible cooling and to attain thermal comfort.

Similarly, the ambient air enters the regeneration side at stage 5. In the next stage 5–6, air passes through a direct evaporative cooler. During this process, the air is cooled due to evaporative cooling effect. Later, at

Table 4
Design parameters of desiccant and heat recovery wheel.

Sr. #	Parameters	Values
Properties of desiccant wheel		
1	Wheel material	Silica gel
2	Model no.	ECDS-151210–17
3	Total cross section area	0.11 m^2
4	Process zone area	0.50
5	Diameter of wheel	0.370 m
6	Dehumidification capacity system (Reg. temp = 70 °C, flow of air = 800 kg/hr.)	0.4
7	Thickness of wheel	0.20 m
Heat Recovery Wheel		
1	Material	Aluminium
2	Diameter of wheel	0.37 m
3	Thickness of wheel	0.20 m
4	Sensible efficiency	0.750
5	Capacity of air handling	450.0cfm

stages 6–7 the regeneration side air is passed through the heat recovery wheel and goes through sensible heating. Afterwards, it passes through water to air heat exchanger for rising the air temperature so that it can regenerate the desiccant wheel. Finally, the return air is passed through the desiccant wheel to absorb the moisture content and restore the desiccant wheel for the next cycle to continue the dehumidification operation.

2.5.3. TRNSYS simulation model of SDI-MC

Fig. 6 demonstrates the SDI-MC model developed in TRNSYS software. Different control strategies are adopted for efficiently harnessing solar thermal energy. TMY Weather data of Taxila Pakistan that is characterized as hot and humid climate is used in annual transient simulation.

Similarly, the information flow diagram of TRNSYS Model is shown in Fig. 7 by connecting various critical components of the SDI-MC system. This model is used to simulate the performance of three different types of collectors, including evacuated tubes, parabolic troughs, and flat plate collectors.

Desiccant and heat recovery wheel design parameters are described in Table 4. The material used for the desiccant wheel is silica gel. Similarly, the heat recovery wheel is made up of Aluminum as it is non-toxic and corrosion resistant.

Table 5 provides a description of the essential elements, parameters, and their specifications that are used during the simulation. All components that are used to develop the simulation model are standard components of TRNSYS Library and their complete description can be found in the TRNSYS document [26]. However, the regenerative evaporative cooler known as M−Cycle cooler is regression based mathematical model developed in Engineering Equation Solver and its performance is validated from the comprehensive experimental data obtained from a test rig shown in Fig. 9. The output of various key performance parameters of the simulation model is plotted online, with a convergence value of 0.001, and the successive substitution approach is chosen as the solver scheme. In this model, the convergence mode is 0.001 and the solver arrangements are solved using the successive approach.

Furthermore, control card characteristics of the TRNSYS simulation studio are given in Table 6.

2.6. Simulation design parameters

The design of SDI-MC system model depends upon different parameters such as weather condition, thermal load, and comfort conditions. The system is designed to handle a maximum humidity ratio of 18 g/kg and ambient temperature of 45 °C. The hourly incident solar radiation profile for hot and humid climate of Taxila Pakistan is shown in Fig. 8.

Table 5
Key elements of the simulation model: An overview [26].

Sr. #	TRNSYS Type	Legends	Parameters	Explanation
1	Type 1b	FPC	1. Series no. = 20 2. Area of collector = 40 m^2	Thermal efficiency of a collector
2	Type 71	ETC	1. Series no. = 20 2. Area of collector = 40 m^2	Additional feature to the thermal model as compared to FPC.
3	Type 536	PTC	1. Aperture area = 2 m^2 2. Number in series = 20.0	It is used to concentrate solar radiation.
4	Type 2b	Diff. Controller	3. Oscillation count = 52	Control functions generate range between zeros to one.
5	Type 700	Auxiliary heater	1. Rated capacity = 40 kW 2. Boiler and combustion efficiency are 0.78 % and 0.85 % respectively	To get the desired outlet temperature
6	Type 11d	mix the water	–	It is used as water mixer
7	Type 648	Air mixer	Total no. of ports = 2	To determine the characteristics of the output air, various streams of air are mixed.
8	Type 66a	Desiccant model	Input and output = 5	To determine the properties of process and regeneration air after passing through the desiccant wheel
9	Type 22	Feedback controller	1. No. of oscillations = 7 2. Set point = 0.010 kg/kg	It serves to keep the controlled variable at the target value.
10	Type 667c	Heat wheel	Rated power = 186 W	Recovery of heat from air to air
11	Type 11b	Tempering valve	Allowable no. of oscillations = 7	It is used to control temperature and change flow direction
12	Type 652	Heat exchanger	1. Fluid heat capacity = 4.19 kJ/kg.K 2. Mode = Counter flow	Heat exchange from water to air
13	Type 62	Excel data	Total no. of inputs = 4	Using an Excel sheet to call up experimental data

Table 6
Control card characteristics for the simulation mode.

Sr. #	Characteristics	Value
1	Simulation start time	1hr.
2	Simulated start time	8760hr.
3	Simulating time in steps	1 hr.
4	Integration of intolerance	0.0010
5	confluence of tolerance	0.0010
6	Method of result	Successive Method

The design parameters of the simulation model of building according to room temperature of 25 °C and relative humidity 50 % are described in Table 7.

The specifications of SDI-MC design parameter are described as shown in Table 8. This design is made with respect to the design load and supply parameters.

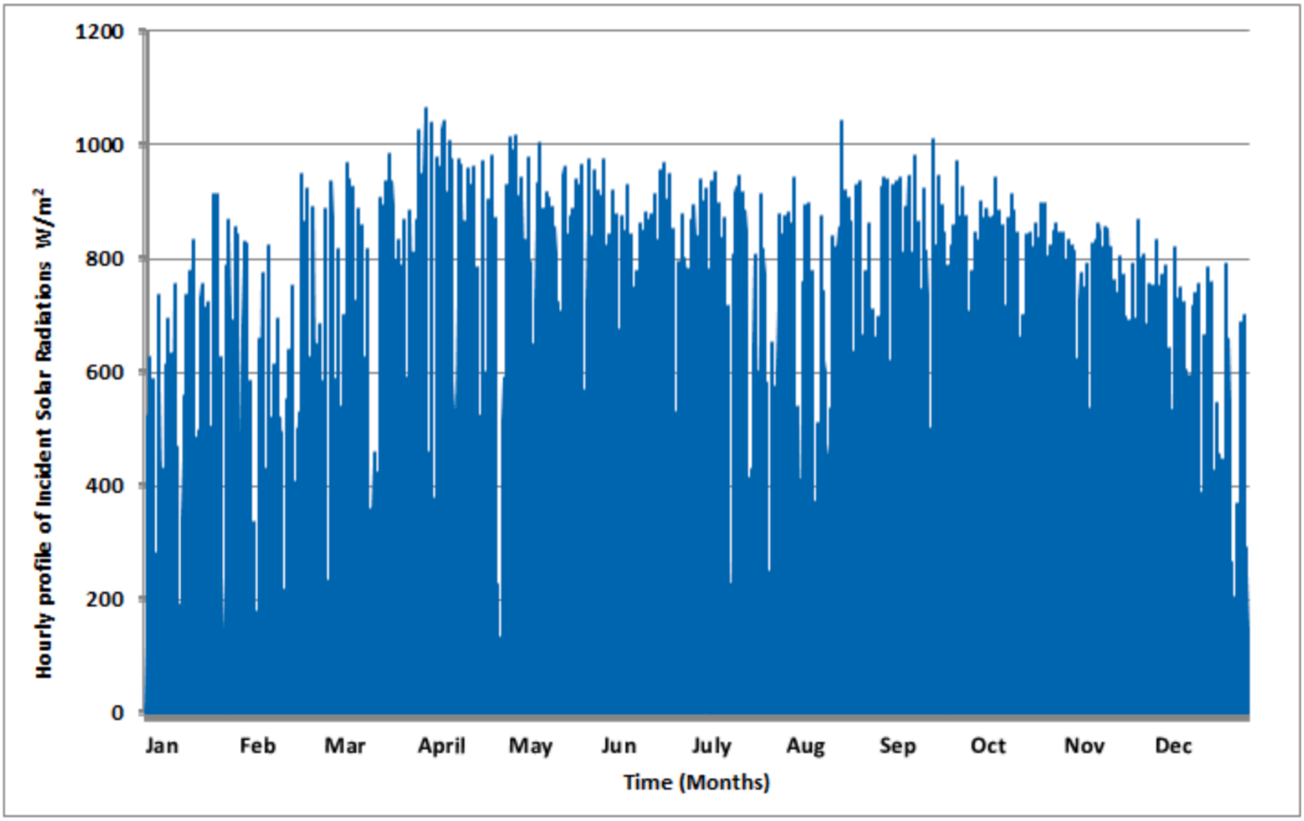

Fig. 8. Hourly profile of incident solar radiations.

Table 7
Design considerations for SDI-MC supply air.

Sr. #	Design parameter	Value
1	Supply air of cooling demand (per ton)	2430 kg/hr.
2	Supply air temperature design	18 °C
3	Supply air humidity air design	10 kg/hr.

Table 8
SDI-MC system design parameters.

Sr. #	Design parameters	Value
1	**Supply and return fans**	
	Flow rate design	6000 kg/hr.
	Consumption of supply fan	2 horsepower
	Power consumption of supply fan	1 horsepower
	Material	Aluminium
	Power consumption of motor	80 W
	Flow rate Design	5000 kg/hr.
2	**Desiccant wheel**	
	Material of wheel	Silica gel
	Flow rate designs	5000 kg/hr.
	Power consumption	80 W
	Rotational speed	20RPH
3	**Spray humidifiers**	
	Saturation efficiency	0.85 %
	Flow rate design	5000 kg/hr.
	Pressure drops of air	235Pascal
	Pump power	70 W

Table 9
Thermodynamic properties of desiccant wheel.

Sr. #	**Parameters**	**Value**
1	material	Silica gel
2	absorbent density	1200 kg/m^3
3	diffusion coefficient	2.27 * 107
4	activation energy	1720 m^2/s
5	specific heat capacity	921 K

Thermodynamic properties of desiccant wheel are described in Table 9.

Finally, design of solar water heating system (SWHS) depends on average annual incident solar radiations, and the air conditioning load of system. According to air conditioning load solar water heating system (SWHS) design parameters are given in Table 10.

2.7. Model validation with experimental data

It is critical to benchmark and evaluate the mathematical models at component as well as system level including desiccant wheel and the innovative evaporative cooling system (M−Cycle) before using them in transient analysis. The simulation model is therefore validated at the component and system levels by the indigenously developed test rig at Renewable Energy Research and Development Center UET Taxila, Pakistan as shown in Fig. 9. During this process the component parameters and other required properties are kept according to the experimental setup and real test conditions respectively. The component and the system performance are assessed against the same parameters as used for experimentation. The design parameters, and range of their variation for model validation are given in Table 11.

The results compared and validated the inlet temperature variation from 30 °C to 3 °C and humidity variation from 10 to 13 g/kg. Three

Table 10
Solar water heating system design specifications.

Sr. #	Design parameter	Value		
1	**Storage tank Reference** [28]			
	Volume of tank	3 m^2		
	Coefficient loss	2.50 W/m^2K		
	Boiling point	230 °C		
	Total number of nodes	5		
	Specific heat of fluid	3.60 J/g°C		
2	**Hot water circulation pump** [29]			
	Maximum flow	2,000,000 g/hr.		
	Power coefficient	0.50		
	Maximum power	200 W		
3	**Auxiliary gas heater** [28]			
	Rated capacity	30.000 W		
	Boiler efficiency	0.78 %		
	Combustion efficiency	0.85 %		
4	**Different solar thermal collectors**			
	Parameter	**Values**		
		FPC [30]	PTC[31]	ETC[32]
	Efficiency	0.75 %	0.67 %	0.83 %
	Maximum operating pressure	10 bar	15 bar	6 bar
	Absorber area	40 m^2	40 m^2	40 m^2
	Slope of collector	33°	45°	33°
	A 1 (WK^{-1} m^{-2})	4.300	–	1.850
	Stagnation temperature	197 °C	250 °C	238 °C
	Slope efficiency	–	15 %	–
	A 2 (WK^{-1} m^{-2})	0.00640	–	0.0070

critical parameters such as inlet and outlet temperature and COP of the system are used to validate the entire model of SDI-MC. In addition, the Excel file contains the experimental data values needed as input for the model. TRNSYS then acquires these values to carry out the execution in a comparable environment.

2.8. Mathematical calculations

The study focuses on several important performance measurements and these parameters are explained below. The following equation (1) [12] is utilized to calculate the sensible cooling capacity.

$$Q_{sen} = \left(\frac{C_p \rho q (T_{sin} - T_{sout})}{3600}\right) \tag{1}$$

By using equation (2) [12] calculate the latent load capacity of the system.

$$Q_{lat} = \left(\frac{H \rho q (\omega_{sin-} \omega_{sout})}{3600}\right) \tag{2}$$

Equation (3) [12] is used to compute the SDI-MC cooling system's sensible heat factor.

$$SHF = \frac{Q_{sen}}{(Q_{sen} + Q_{lat})} \tag{3}$$

The auxiliary energy input and COP of SDI-MC are calculated by the following equations (4) & (5) [12].

$$Q_{reg} = \dot{m}_{reg}(h_7 - h_8) \tag{4}$$

$$COP = \frac{(Q_{sen} + Q_{lat})}{Q_t} \tag{5}$$

Moreover, solar energy gain and thermal efficiency of the three collectors are calculated by equation (6) and (7) [12].

$$Q_{sol} = \dot{m}_{wc} C_{pw} (T_{11} - T_{10}) \tag{6}$$

$$\eta_{s,c} = \frac{\dot{m}_w c_p (T_{w,c,in} - T_{w,c,out})}{GA_c} \tag{7}$$

Table 11
Model Validation of different parameters.

Sr. #	Parameters	Theoretical analysis		Experimental analysis	
		Parametric variations	Baseline values	Parametric variations	Baseline values
1	Ambient air temperature	–	30.0 °C	–	26.0 °C
2	Regeneration air inlet humidity ratio	–	12.50 g/kg	–	12.0 g/kg
3	Process Air inlet Temperature	(20 to 40) °C	31.0 °C	(25 to 45) °C	25.0 °C
4	Rotation Speed	(15 to 36) RPH	15RPH	(10 to 40) RPH	18 RPH
5	Process air Velocity	(1 to 3.5) m/s	2.0 m/s		2.0 m/s
6	Regeneration Air Temperature	(45 to 120) °C	81.0 °C	(50 to 80) °C	80.0 °C
7	Process air Inlet Humidity	(4–12) g/kg	8.0 g/kg	(12–18) g/kg	12 g/kg
8	Ambient air humidity ratio	–	–	–	11 g/kg
9	Process air Velocity	(1 to 3.5) m/s	2.0 m/s	–	m/s

Fig. 9. Experimental test rig of SDI-MC.

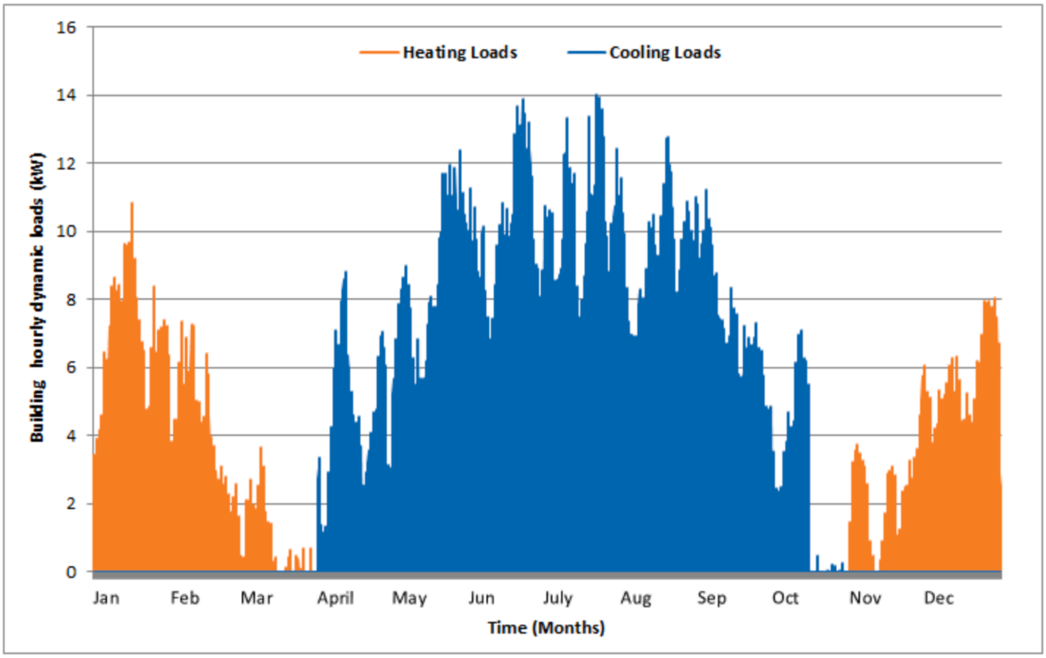

Fig. 10. Building hourly dynamic loads.

Equation (8) [12] can be used to determine how much supplementary energy is needed to reach the specified regeneration temperature.

$$Q_{aux} = \dot{m}_{wds} C_{pw} (T_{13} - T_{14}) \tag{8}$$

Furthermore, equations (9) and (10) [12] are used to determine the auxiliary energy share and total thermal energy input.

$$AES = 1 - SF \tag{9}$$

$$Q_t = Q_{sol} + Q_{aux} \tag{10}$$

Finally, the cooling system's root mean square error value and the system's solar fraction are calculated by equations (11) and (12) [12].

$$RMSE = \sqrt{\frac{\sum_{i=1}^{n} (X_{exp} - X_{model})^2}{n}} \tag{11}$$

$$SF = \frac{Q_{sol}}{(Q_{sol} + Q_{aux})} \tag{12}$$

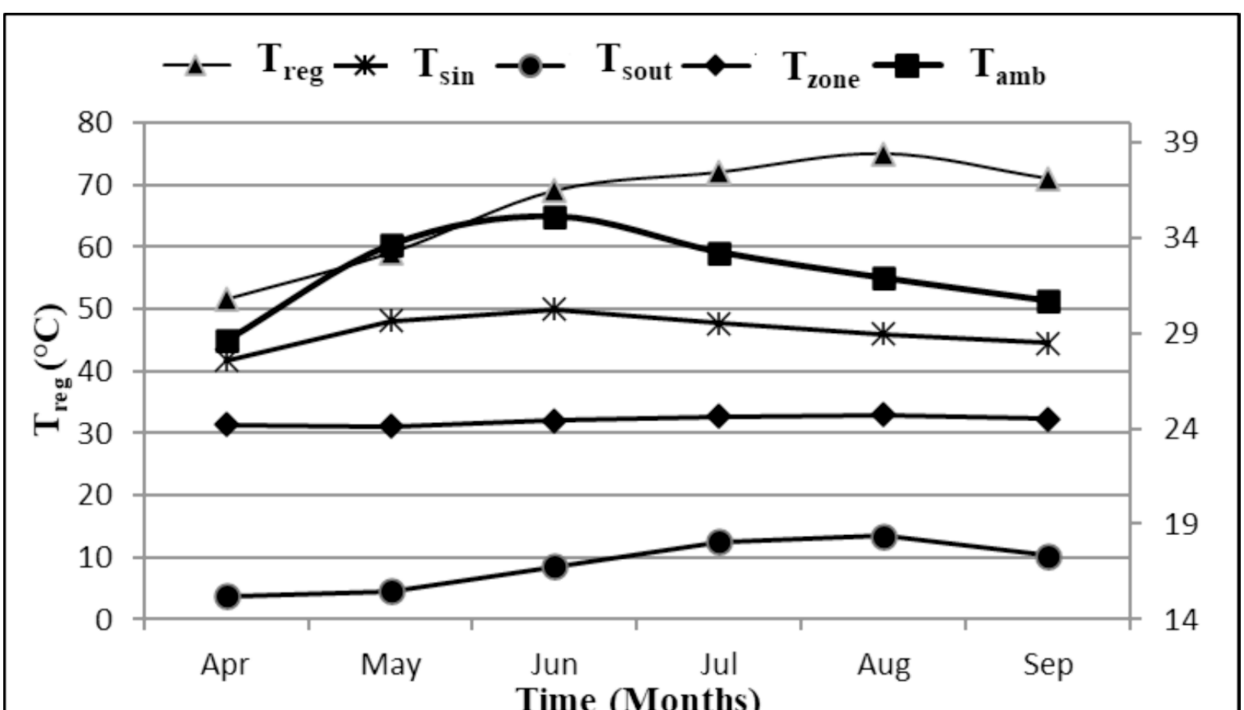

Fig. 11. SDI-MC system and zone temperature.

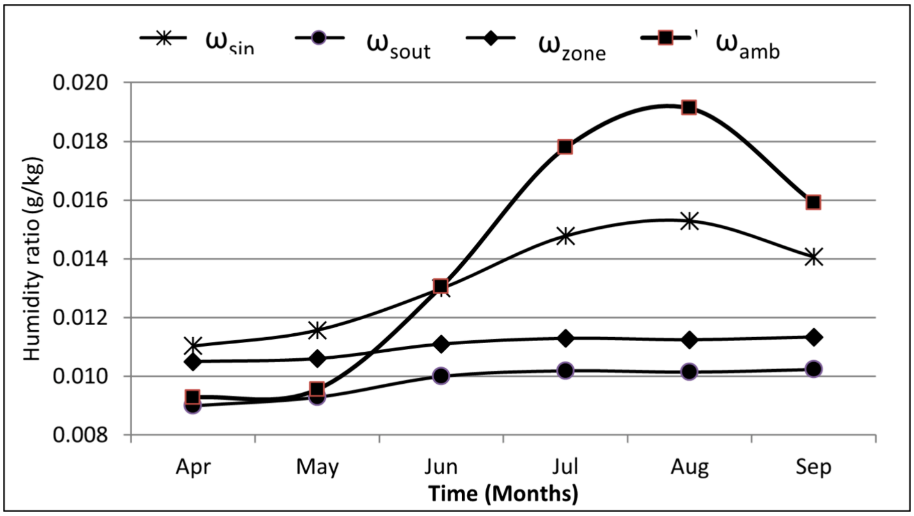

Fig. 12. Variation of air humidity ratio over time.

3. Result and discussions

Annual transient seasonal analysis of the SDI-MC system was conducted using TRNSYS software with various solar collectors in hot and humid climate of Taxila Pakistan. An important discussion on the important performance parameters is summarized in subsequent sections.

3.1. Building dynamic air-conditioning loads

The building dynamic air-conditioning loads are shown in Fig. 10. The heating loads are observed from January to mid of March and from November to December. The maximum heating occurs in January, and it is 8.8 kW. Similarly, cooling season is observed from April to October with maximum cooling demand of 14 kW.

3.2. Temperature profile of cooling system and building zones

The results of the solar desiccant integrated Maisotsenko cycle cooling system on monthly average basis are described in Fig. 11. Initially, the regeneration temperature demand is low from April to July as moisture content of the ambient air is low. However, as the August is characterized as monsoon season in Pakistan, where humidity of ambient air is enhanced and reaches up to 18 g/kg of air. Therefore, regeneration temperature demand is highest in August. Similarly, the highest ambient temperature of 37 °C exists in June. However, despite of high inlet temperatures the systems regeneration temperature demand lies around 70 °C. This shows that the system performance is strongly affected by the humidity of inlet air and less affected by the inlet temperatures.

3.3. Performance of system subjected to various humidity ratio

The monthly average values of humidity ratio are shown in Fig. 12. The humidity ratio in the zone varies from 10 g/kg to 11 g/kg that confirms the ASHRAE standard of maintaining the humidity ratio below 12 g/kg. It can be seen that, from April to July, there is a gradual increase in inlet humidity, with the peak value of 14.0 g/kg being recorded in August when ambient air humidity ratio reaches up to 19 g/kg. Moreover, these results indicate that the overall system has achieved satisfactory thermal comfort levels.

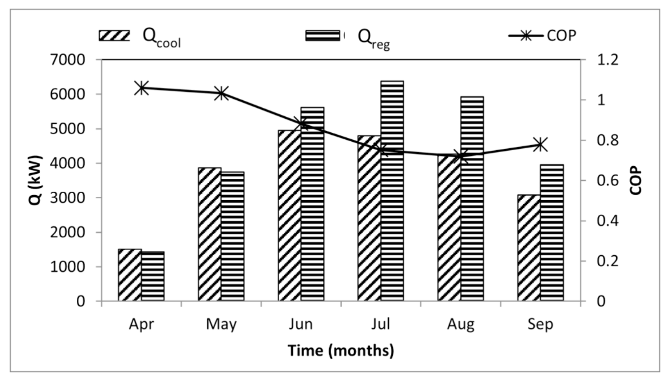

Fig. 13. Variation of COP along with cooling, and regeneration, loads.

3.4. COP of the system

The monthly variation in the COP of the SDI-MC system is shown in Fig. 13. The highest COP of the system, which is observed to be 1.13, occurs in April, while the minimum COP of 0.78 occurs in August due to fact that April is characterized by low humidity of ambient air and requires low regeneration energy for the desiccant wheel regeneration, while August is characterized by highest ambient moisture content that reaches up to 19 g/kg, therefore it requires higher regeneration energy and in turns lowers the COP of the system.

3.5. Thermal efficiency of solar collectors

A substantial relationship between the two variables is seen in Fig. 14, which shows how collector efficiency changes in relation to average solar radiation. The ETC, which reached a peak value of 55 % in August, is the most effective of the three sources. While FPC and PTC reach their peak efficiency in June with corresponding values of 35 % and 37 %, respectively.

Despite the fact that the solar radiation trends show that it is maximum in May and collector efficiency is highest in July. It is due to the fact that regeneration thermal energy requirement in the month of July is higher, and the system has to deal with maximum latent load of dehumidification. Therefore, due to higher demand of solar thermal energy the solar system thermal energy gain is high and as a result collector efficiency is also maximum.

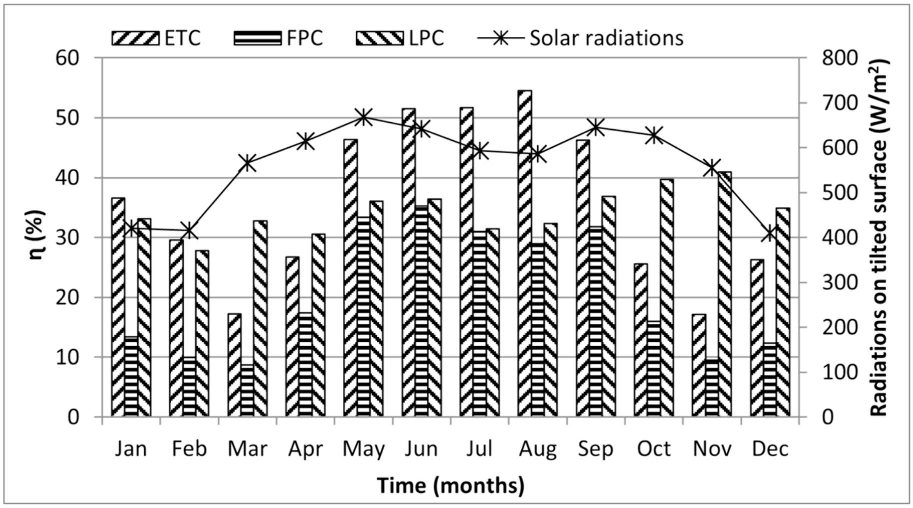

Fig. 14. Profile of monthly collector's efficiency.

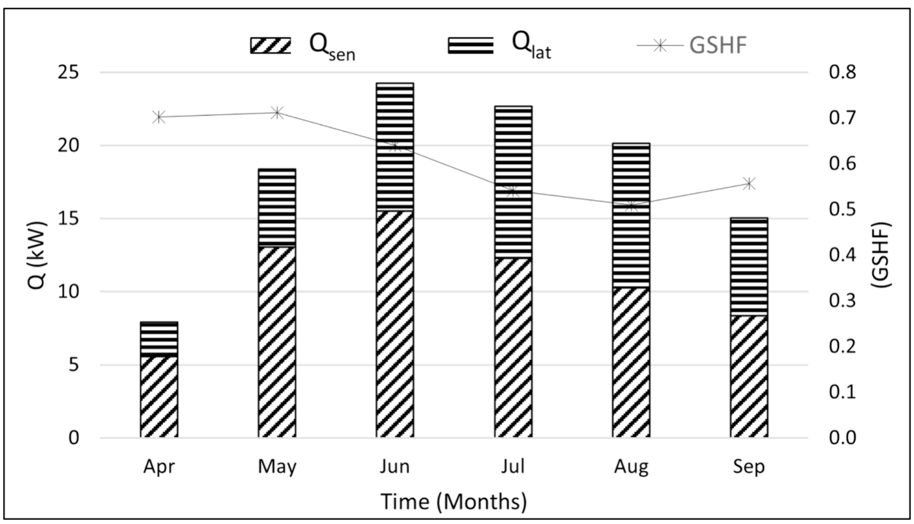

Fig. 15. Variations of air conditioning loads.

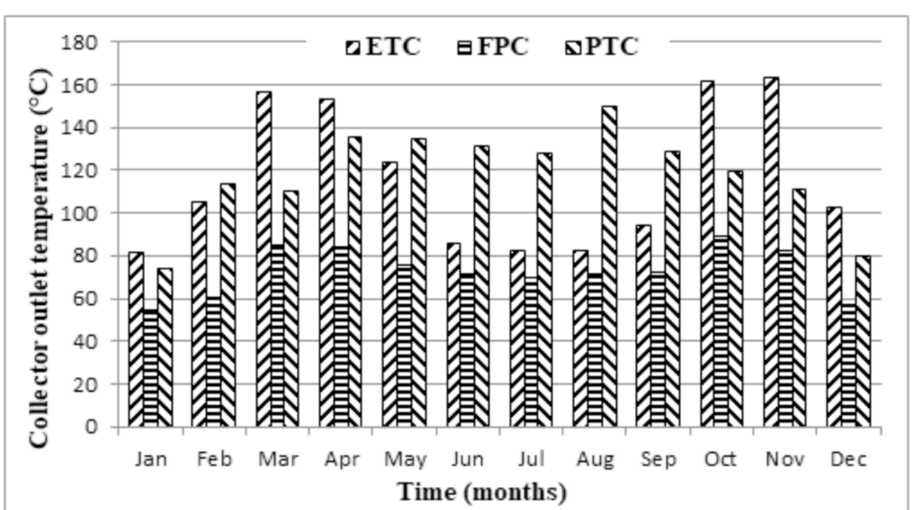

Fig. 16. Variation in collector's outlet temperature.

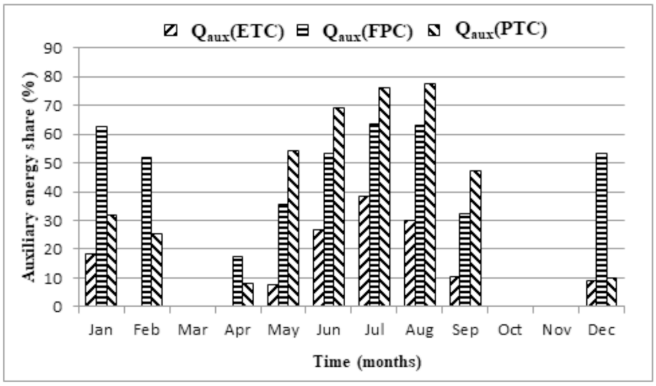

Fig. 17. Auxiliary energy demands.

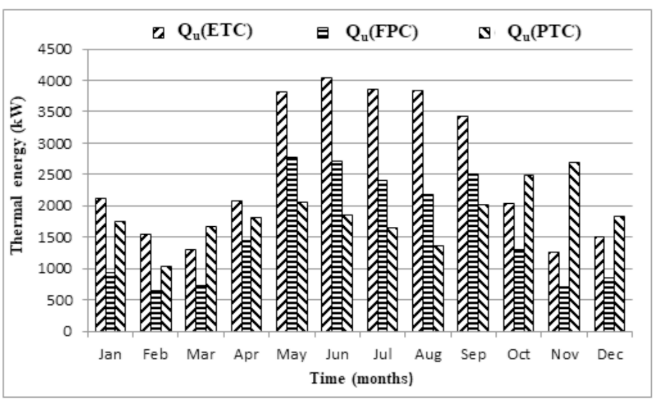

Fig. 18. Useful energy output from different solar collectors.

3.6. Evaluating the cooling performance of the SDI-MC system

The variation in the grand sensible heat factor (GSHF) along with sensible and latent loads is shown in Fig. 14. Its minimum observed average value is 0.55 in August when the system handles maximum latent loads of about 8 kW as July is characterized by the highest moisture content in the ambient air. Whereas the maximum reported value of GSHE is 0.6 in April when ambient air humidity and latent loads of air-conditioning is low. The DAC system can be used in subtropical conditions due to its lower values of GSHF.

3.7. Collectors outlet temperatures

Variation of collector outlet temperatures is shown in Fig. 16. The tilt angle of the flate plate and evacuated tube collector is maintained at 33°. The results revealed that the maximum monthly average temperatures occur for evacuated tube collector reaching up to 160 °C and proves to be the most efficient and suitable collector technology for solar thermal air-conditioning.

3.8. Investigating auxiliary energy consumption for effective SWHS

As solar energy is intermittent in nature, it requires an auxiliary energy source for its continuous operation. The auxiliary energy requirement for operating SDI-MC is shown in Fig. 17 and it can be observed that it is highest for flat plate collector followed by parabolic trough collector due to its low thermal efficiency.

3.9. Analysis of useful energy gain from solar collectors

Fig. 18 demonstrates the annual solar energy gains achieved by utilizing three different types of solar thermal collectors. It is observed that evacuated tube collectors have the highest energy gain, which is 4000 kW during June. However, the energy gained from PTC during the winter season is higher as compared to flat plate collectors as the thermal energy loss is high in flat plate collector while parabolic trough collector uses evacuated tube as receiver.

3.10. Evaluating the validity of SDI-MC model simulation with experimental data

To validate the experimental results, TRNSYS model of SDI-MC system as discussed in section 2.5.3 is simulated against the same parameters as used for the experimentation.

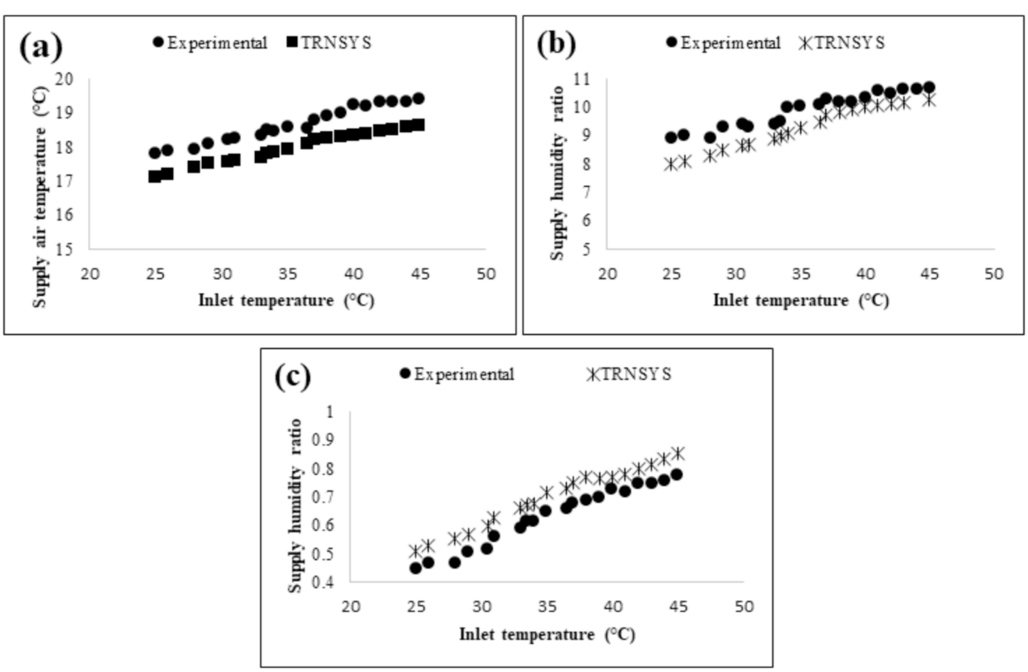

Fig. 19. Comparative evaluation of experimental data and TRNSYS model outputs for SDI-MC system.

Fig. 19 shows the comparison of experimental and TRNSYS model results in term of supply air temperature, supply air humidity ratio and COP of the SDI-MC system TRNSYS model is simulated against the inlet parameters; inlet ambient temperature 25–45 °C, inlet humidity ratio 14 g/kg, regeneration temperature 70 °C, return air conditions 27 °C and 12.5 g/kg and air flow rate of 660 kg/hr [19]. It can be observed that the experimental results are in good agreement with RMSE of 0.7 °C, 0.6 kg/kg, and 0.1 for outlet temperature, supply humidity ratio, and COP respectively.

4. Conclusions

The study of SDI-MC under transient conditions found that the system's performance is significantly impacted by ambient conditions. A rise in ambient temperature results in an increase in the system's COP. The cooling system's COP for SDI-MC varies between 0.78 and 1.13. In April, the system has a maximum cooling capacity of 24 kW with a SHF factor of 0.720. The dehumidification effectiveness ranges from 29 % to 49 % and decreases remarkably with an increase in inlet temperature but improves with a rise in inlet humidity. The outlet water temperature and its temperature gradient are strongly influenced by solar irradiance. The results of the study indicate that the evacuated tube collector has the highest annual efficiency at 35.80 %, followed by the parabolic trough at 34.39 % and the flat plate collector at 20.65 %. Additionally, the evacuated tube collector has the highest annual energy gain of 2606 kW, while the parabolic trough and flat plate collector have 1885 kW and 160 kW respectively. The flat plate collector requires the highest annual auxiliary energy share at 37.08 %, whereas the parabolic trough and evacuated tube collector require 34.16 % and 12.5 %, respectively.

Funding

Muhammad Waheed Azam has a PhD fellowship in the framework of PON R&I 2014/2020 (CCI 2014IT16M2OP005), Action IV.5- "PhD on green issues", funded by the Ministry of University and Research (MUR), Italy, FSE-REACT-EU.

CRediT authorship contribution statement

Ghulam Qadar Chaudhary: Writing – original draft, Visualization, Validation, Investigation, Supervision, Conceptualization, Writing – review & editing. **Muhammad Waheed Azam:** Writing – original draft, Visualization, Validation, Software, Methodology, Formal analysis, Data curation. **Fabio Bozzoli:** Writing – review & editing, Formal analysis, Supervision, Investigation. **Uzair Sajjad:** Writing – review & editing, Visualization, Investigation, Formal analysis. **Pamela Vocale:** Writing – review & editing. **Luca Cattani:** Writing – review & editing, Conceptualization, Software. **Rasoul Fallahzadeh:** Writing – review & editing, Conceptualization.

Declaration of competing interest

The authors declare that they have no known competing financial interests or personal relationships that could have appeared to influence the work reported in this paper.

Data availability

Data will be made available on request.

References

[1] Pérez-Lombard L, Ortiz J, Pout C. A review on buildings energy consumption information. Energy Build 2008;40(3):394–8.
[2] Jani DB, Mishra M, Sahoo PK. Solid desiccant air conditioning – A state of the art review. Renew Sustain Energy Rev 2016;60:1451–69.
[3] Liu Y, Akhlaghi YG, Zhao X, Li J. Experimental and numerical investigation of a high-efficiency dew-point evaporative cooler. Energy Build 2019;197:120–30.
[4] Liberty JT, Ugwuishiwu BO, Pukuma SA, Odo CE. Principles and application of evaporative cooling systems for fruits and vegetables preservation. Int J Curr Eng Technol 2013;3(3):1000–6.
[5] Hussain I, et al. Evaluating the parameters affecting the direct and indirect evaporative cooling systems. Eng Anal Bound Elem 2022;145(September):211–23. https://doi.org/10.1016/j.enganabound.2022.09.016.
[6] M.D. Borasiya, P.N. Kher, V.H. Atodariya, "A Review on Potential of Indirect Evaporative Cooling System," 2017;3(9):170–5.
[7] Sadighi Dizaji H, Hu EJ, Chen L. A comprehensive review of the Maisotsenko-cycle based air conditioning systems. Energy 2018;156:725–49.
[8] Cui X, Tian W, Yang X, Kong Q, Chai Y, Jin L. Experimental study on a crossflow regenerative indirect evaporative cooling system. Energy Procedia 2018;152:395–400.
[9] Pandelidis D, Anisimov S, Worek WM. Numerical analysis of a desiccant system with crossflow maisotsenko cycle heat and mass exchanger. Energy Build 2016;123:136–50.
[10] Kanti PK, Sharma P, Maiya MP, Sharma KV. The stability and thermophysical properties of Al_2O_3-graphene oxide hybrid nanofluids for solar energy applications: application of robust autoregressive modern machine learning technique. Sol Energy Mater Sol Cells 2023;253(February):112207. https://doi.org/10.1016/j.solmat.2023.112207.
[11] Said Z, Rahman S, Sharma P, Amine Hachicha A, Issa S. Performance characterization of a solar-powered shell and tube heat exchanger utilizing MWCNTs/water-based nanofluids: an experimental, numerical, and artificial intelligence approach. Appl Therm Eng 2022;212(May):118633. https://doi.org/10.1016/j.applthermaleng.2022.118633.
[12] Gopi A, Sharma P, Sudhakar K, Ngui WK, Kirpichnikova I, Cuce E. Weather impact on solar farm performance: A comparative analysis of machine learning techniques. Sustainability 2023;15(1). https://doi.org/10.3390/su15010439.
[13] Vivekh P, Bui DT, Islam MR, Zaw K, Chua KJ. Experimental performance evaluation of desiccant coated heat exchangers from a combined first and second law of thermodynamics perspective. Energy Convers Manag 2020;207(January):112518.
[14] Delfani S, Karami M. Transient simulation of solar desiccant/M-Cycle cooling systems in three different climatic conditions. J Build Eng 2020;29(December 2019):101152.
[15] Samad A, Waheed A, Bilal M, Fatima M, Zahra A, Siddiqui MS. Dynamic simulation and parametric analysis of solar assisted desiccant cooling system with three configuration schemes. Sol Energy 2020;197(December 2019):22–37.
[16] Kalogirou SA. Use of TRNSYS for modelling and simulation of a hybrid pv – thermal solar system for Cyprus. Renew Energy 2001;23:247–60.
[17] Ma Y, Guan L. Performance analysis of solar desiccant-evaporative cooling for a commercial building under different Australian climates. Procedia Eng 2015;121:528–35.
[18] Khalid A, Mahmood M, Asif M, Muneer T. Solar assisted, pre-cooled hybrid desiccant cooling system for Pakistan. Renew Energy 2009;34(1):151–7.
[19] Qadar Chaudhary G, Ali M, Sheikh NA, Gilani SI, Khushnood S. Integration of solar assisted solid desiccant cooling system with efficient evaporative cooling technique for separate load handling. Appl Therm Eng 2018;140(April):696–706.
[20] Bourdoukan P, Wurtz E, Joubert P. Experimental investigation of a solar desiccant cooling installation. Sol Energy 2009;83(11):2059–73.
[21] Comino F, González JC, Navas-martos FJ, De Adana MR. Experimental energy performance assessment of a solar desiccant cooling system in Southern Europe climates. Appl Therm Eng 2020;165(October 2019):114579.
[22] Jani DB, Mishra M, Sahoo PK. Performance prediction of rotary solid desiccant dehumidifier in hybrid air-conditioning system using artificial neural network. Appl Therm Eng 2016;98:1091–103.
[23] Munusamy A, Barik D, Sharma P, Medhi BJ, Bora BJ. Performance analysis of parabolic type solar water heater by using copper-dimpled tube with aluminum coating. Environ Sci Pollut Res 2023. https://doi.org/10.1007/s11356-022-25071-5.
[24] Asim M, Dewsbury J, Kanan S. TRNSYS simulation of a solar cooling system for the hot climate of Pakistan. Energy Procedia 2016;91:702–6.
[25] Jani DB, et al. A review on use of TRNSYS as simulation tool in performance prediction of desiccant cooling cycle. J Therm Anal Calorim 2020;140(5):2011–31. https://doi.org/10.1007/s10973-019-08968-1.
[26] Klein SA, Beckman WA, Duffie JA. Trnysys - a transient simulation program. ASHRAE Trans 1976;82(pt 1):623–33.
[27] Jaelani A, Kusumah YS, Turmudi. The design of sketchup software-aided generative learning for learning geometry in senior high school. J. Phys. Conf. Ser 2019;1320(1). https://doi.org/10.1088/1742-6596/1320/1/012048.
[28] Pakistan Standard (2021). Storage Gas Water Heater/Geyser ICS: NO.97.100.20: 91.140.65. https://www.psqca.com.pk/.
[29] Hot water circulation pump. https://acquaer.com/collections/hot-water-circulation-pump.html.
[30] Solar water heaters - solar water heating. Northern Lights Solar Solutions. (n.d.). https://www.solartubs.com/flat-plate-solar-specs.html.
[31] Chaudhary GQ, Kousar R, Ali M, Amar M, Amber KP, Lodhi SK, et al. Small-sized parabolic trough collector system for solar dehumidification application: design. Int J Photoenergy 2018;2018:5759034.
[32] Sunmax solar. https://www.sunmaxxsolar.com/product/20-evacuated-tube collector.html.